The Role of ATF4 Stabilization and Autophagy in Resistance of Breast Cancer Cells Treated with Bortezomib

Manuela Milani,[1] Tomasz Rzymski,[1] Howard R. Mellor,[1] Luke Pike,[1] Alberto Bottini,[2] Daniele Generali,[2] and Adrian L. Harris[1]

[1]Growth Factor Group, Cancer Research UK, Molecular Oncology Laboratories, Weatherall Institute of Molecular Medicine, University of Oxford, John Radcliffe Hospital, Headington, Oxford, United Kingdom and [2]Breast Unit, Istituti Ospitalieri Cremona, Cremona, Italy

Abstract

The ubiquitin-proteasome system plays a key regulatory role in cellular homeostasis. The inhibition of the 26S proteasome by Bortezomib leads to the accumulation of misfolded proteins, resulting in endoplasmic reticulum stress followed by a coordinated cellular response called unfolded protein response (UPR). Endoplasmic reticulum stress is also a potent inducer of macroautophagy. Bortezomib is a selective and potent inhibitor of the 26S proteasome and is approved for the treatment of multiple myeloma. Clinical trials with Bortezomib have shown promising results for some types of cancers, but not for some others, including those of the breast. In this study, we show that Bortezomib induces the UPR and autophagy in MCF7 breast cancer cells. Surprisingly, Bortezomib did not induce phosphorylation of PERK, a key initial step of the UPR. We show that induction of autophagy by Bortezomib is dependent on the proteasomal stabilisation of ATF4 and up-regulation of LC3B by ATF4. We show that ATF4 and LC3B play a critical role in activating autophagy and protecting cells from Bortezomib-induced cell death. Our experiments also reveal that HDAC6 knockdown results in decreased LC3B protein and reduced autophagy. Our work shows that the induction of autophagy through ATF4 may be an important resistance mechanism to Bortezomib treatment in breast cancer, and targeting autophagy may represent a novel approach to sensitize breast cancers to Bortezomib. [Cancer Res 2009;69(10):4415–23]

Introduction

The ubiquitin-proteasome pathway plays a key regulatory role in cellular homeostasis through the degradation of multiple proteins implicated in the regulation of cell growth and apoptosis. The 26S proteasomes are multicatalytic protease complexes consisting of a 20S catalytic core and regulatory 19S subunit, responsible for most nonlysosomal intracellular degradation (1).

The dipeptide boronic acid Bortezomib is a selective and potent inhibitor of the 26S proteasome that reversibly inhibits the proteasomal chymotrypsin-like activity (1). Preclinical studies showed a broad antitumor activity of Bortezomib, and numerous clinical trials are currently investigating its efficacy as a single agent and in combination with other active antitumor agents against a variety of malignancies (2). Although Bortezomib is now approved for the treatment of multiple myeloma, clinical experience with Bortezomib has shown limited activity against solid tumors, including those of the breast, when used as a single agent (3).

The inhibition of the 26S proteasome by Bortezomib may lead to the accumulation and aggregation of misfolded proteins in the endoplasmic reticulum lumen resulting in activation of the unfolded protein response (UPR), through the action of three key endoplasmic reticulum–resident transmembrane proteins, PERK, IRE1, and ATF6 (4–6). PERK is a member of a family of protein kinases that phosphorylates the α subunit of the cytosolic eukaryotic translation initiation factor eIF2α, resulting in a reduced global protein synthesis and in a preferential translation of selected mRNAs including *Activating Transcription Factor 4* (*ATF4;* refs. 5, 6). ATF4 orchestrates a gene expression program involved in oxidative stress, amino acid synthesis, differentiation, metastasis, and angiogenesis known as integrated stress response (5, 6). The UPR leads to simultaneous activation of both adaptive and proapoptotic pathways. One of the best characterized of these pathways is mediated by cyclophosphamide-Adriamycin-vincristine-prednisone (CHOP; Oncovin)/GADD153 a transcription factor, regulated by ATF4, which activates the transcription of *GADD34,* which interacts with protein phosphatase I to catalyze eIF2α dephosphorylation (5).

Previous reports have identified endoplasmic reticulum stress and the eIF2α/PERK pathway as potent inducers of macroautophagy where it promotes cell survival (7, 8); however, the molecular mechanism is not yet clear (9, 10). Autophagy is an evolutionarily conserved caspase-independent process, responsible for the degradation and recycling of long-lived proteins and cytoplasmic-damaged organelles (11). Autophagy begins in the cytoplasm with formation of double membrane vesicles, known as autophagosomes that sequester cytoplasmic material, including organelles and fuse with lysosomes where the contents are degraded by acidic lysosomal hydrolases. Microtubule-associated protein 1 light chain 3B (LC3B) is one of the key factors in autophagosome formation. During autophagy, LC3-I is cleaved and conjugated to phosphatidylethanolamine to form LC3-II, which is associated with the preautophagosomal structures (12).

Although autophagy occurs at basal levels playing a critical role in maintaining cellular homeostasis, it is also involved in many physiologic and pathologic processes (12). Recently, autophagy emerged as a multifunctional pathway activated in response to microenvironmental stress, intracellular damage caused by hypoxia, chemotherapeutic agents, virus infections, and toxins. Autophagy may also have a role in cell death and, as cancer cells often develop mutations that confer resistance to apoptosis, nonapoptotic forms of programmed cell death might be target for novel approaches (11, 12).

Note: Supplementary data for this article are available at Cancer Research Online (http://cancerres.aacrjournals.org/).

Requests for reprints: Adrian L. Harris, Cancer Research UK, Molecular Oncology Laboratories, Oxford, OX3 9DS, United Kingdom. Phone: 44-1865-222457; Fax: 44-1865-222431; E-mail: aharris.lab@imm.ox.ac.uk.

doi:10.1158/0008-5472.CAN-08-2839

It has been shown that autophagy can act as a compensatory degradation system when the UPS is impaired by genetic mutations in *Drosophila*, and that histone deacetylase 6 (HDAC6), a microtubule-associated deacetylase that interacts with polyubiquitinated proteins, is an essential mechanistic link in this compensatory interaction. Inhibition of both the proteasome and HDAC6 by tubacin induced accumulation of ubiquitinated proteins and toxicity in multiple myeloma cells (13–15).

Here, we have investigated the ability of Bortezomib to induce the UPR and autophagy and their role in resistance to Bortezomib in MCF7 breast cancer cells. We have identified autophagy as an important resistance mechanism to Bortezomib treatment in breast cancer and shown that ATF4 stabilisation is a key component of this response. Targeting autophagy may represent a novel approach to sensitize breast cancers to Bortezomib.

Materials and Methods

Cells. The human breast cancer cell lines MCF7 and MDA MB 231 were provided by Cancer Research UK. Cells were maintained in DMEM (with 4.5 mg/mL glucose) supplemented with 10% (vol/vol) FCS, penicillin (100 U/mL) and streptomycin (100 μg/mL), and 4 mmol/L L-glutamine (Life Technologies).

Compounds. Bortezomib was a gift from Millennium Pharmaceuticals, Inc. MG115, MG132, Thapsigargin, and Tunicamycin were from Calbiochem. Cobalt Chloride was from Sigma.

siRNA treatment of cells and transfection procedures. Transfections of siRNA duplexes diluted to give a final concentration of 20 nmol/L in Opti-Mem I (Invitrogen Life Technologies) were performed with cells at 30% to 40% confluency using 24 μL Oligofectamine transfection reagent (Invitrogen).

Immunoblot analysis. Cells were lysed in M-PER buffer (Pierce) supplemented with Complete mini-protease inhibitor cocktail tablets (Roche Diagnostics) and phosphatase/kinase inhibitor cocktail (Sigma). Whole cell lysates were resolved by SDS-PAGE, electroblotted onto polyvinylidene difluoride membrane (Millipore), and probed with the indicated antibodies. Horseradish peroxidase–conjugated anti-rabbit or anti-mouse, goat or mouse secondary antibodies (Dako Irc.) were used with ECL Plus system (Amersham Biosciences) to visualize immunoreactive bands. Proteins were detected using antibodies according to manufacturer's instructions. The mouse monoclonal antibody to HIF1α was from BD Biosciences, the rabbit polyclonal antibodies to ATF4 was from Santa Cruz Biotechnology, the mouse monoclonal to CHOP and mouse monoclonal to eIF2α and the rabbit monoclonal to PERK were from Abcam, the rabbit monoclonal to phospho-eIF2α and the rabbit polyclonal to HDAC6 were from Cell Signaling, the rabbit polyclonal to phospho-PERK was from Biolegend, the mouse monoclonal antibody to MAP1LC3 was from NanoTools, the mouse monoclonal β-tubulin antibody was from Sigma, and the mouse monoclonal β-actin antibody was from Sigma.

Real-time quantitative PCR. In Real-Time Quantitative PCR experiments, the methods used by us for extraction, quantification, and evaluation of the quality of RNA were as previously described (16). cDNA was synthesized by using the High Capacity cDNA Archive kit (Applied Biosystem). qPCR assay and relative quantification of gene expression were performed on the basis of the method described by Pfaff (2001).

Immunochemistry. Cells were grown as monolayers on coverslips. Cells were fixed in −20°C cold methanol for 15 min, washed thrice with PBS, and blocked with 1% bovine serum in PBS (pH 7.5) for 30 min followed by overnight incubation with primary antibody at 4°C. Secondary fluorescent FITC or Cy_3 (Dako) was used at dilution 1:500 in blocking buffer for 1 h. Cells were visualized by using a Nikon microscope fitted with the appropriate filters.

LysoTracker staining. LysotrackerRed fluorescent dye (Invitrogen) was used on cells grown in monolayer according to the manufacturer's instructions. Cells were briefly washed thrice with fresh medium and visualized using a Nikon microscope fitted with the appropriate filters.

Proliferation MTS assay. Proliferation MTS assay was performed by using The CellTiter 96 AQ_{ueous} Non-Radioactive Cell Proliferation Assay (Promega) according to manufacturer's instructions. The absorbance of the formazan at 490 nm was measured directly from 96-well assay plates without additional processing.

Cell counting. Cell counting was performed with BECKMAN COULTER Z Series system.

Fluorescence-activated cell sorting analysis. The assay was performed using the fluorescence-activated cell sorting (FACS) analyzer Cyan ADP (Dako). Annexin V, Alexa Fluor 647, and propidium iodide were from Invitrogen; Annexin V binding buffer was from BD Pharmingen. The data were analyzed using Summit Version 4.3 software.

Results

Induction of UPR and autophagy in MCF7 breast cancer cells. Bortezomib increased the phosphorylation of eIF2α and induced ATF4 protein levels in a dose-dependent (Fig. 1*A*) and time-dependent manner (Fig. 1*B*). Also, mRNA levels of endoplasmic reticulum stress markers including *CHOP*, *GADD34*, and *SKIP3* were significantly increased in Bortezomib-treated cells in a dose-dependent (Fig. 1*C*) and time-dependent manner (Fig. 1*D*) and followed induction of ATF4, as measured by quantitative reverse transcription-PCR (qPCR). For example, after 24 hours of treatment with Bortezomib at the lowest concentration tested (100 nmol/L), *SKIP3* was induced 9-fold, *GADD34* was induced 40-fold, and *CHOP* was induced 20-fold (Fig. 1*C*). Bortezomib treatment also induced protein levels of HIF1α (Fig. 1*A* and *B*); however, mRNA levels of the HIF1α target gene-*BNIP3* were only induced 2- to 3-fold (Fig. 1*C*) or <50% (Fig. 1*D*), consistent with previous reports (17–19) that the form of HIF1α induced by proteasome inhibition is nonfunctional.

Previously, we identified LC3B a key component of the autophagosome, as a protein specifically induced by endoplasmic reticulum stress in an ATF4-dependent manner under severe hypoxia. We next investigated changes of LC3B expression in MCF7 cells treated with Bortezomib. During Bortezomib treatment, LC3B protein and mRNA levels increased significantly in a dose- and time-dependent manner (Fig. 1*A, B, C*, and *D*), and there was an increase in the processed form of LC3B (LC3II), indicative of increased autophagy, particularly at 12 and 24 hours. Also, induction of ATF4 and LC3B in a time-dependent manner was observed in MDA MB 231 cells (Fig. 1*B*).

Differential effects on ATF4 induction by drugs inducing UPR. We next compared the effect of Bortezomib induction of the UPR, ATF4, and LC3B, to other small-molecule inducers of endoplasmic reticulum and cellular stress. The compounds tested included the proteasomal inhibitors MG115, MG132, and Bortezomib, inhibitor of glycosylation Tunicamycin, an inhibitor of Ca^{2+}-dependent endoplasmic reticulum pump Thapsigargin, the oxidative stress-inducer Arsenite, the hypoxia mimetic compound $CoCl_2$, and an iron chelator Desferoxamine. Both of the endoplasmic reticulum stress inducers (Tunicamycin and Thapsigargin) induced ATF4 and LC3B; however, the strongest induction of ATF4 occurred in cells treated with the proteasome inhibitors MG115, MG132, and Bortezomib (Fig. 2*A*). Although levels of phospho-PERK and phospho-eIF2α were similar for all UPR stimuli (Fig. 2*A*), the greater induction of ATF4 suggested that proteasomal stabilization was the main mechanism of ATF4 up-regulation. There was no induction of LC3B or ATF4 in cells treated with Desferoxamine and $CoCl_2$, showing that HIF1α was not involved in ATF4 and LC3B induction (Fig. 2*A*). To further investigate the role

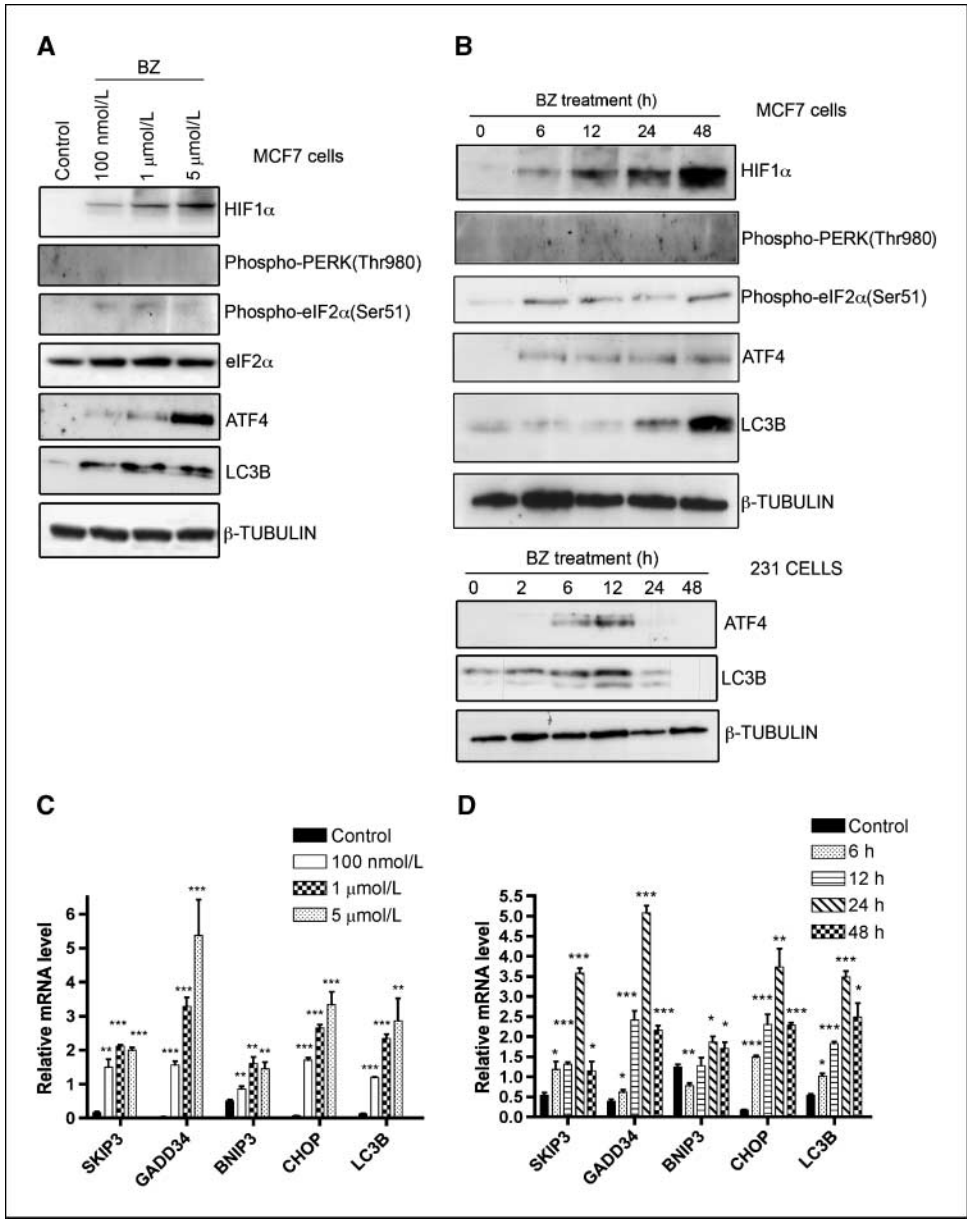

Figure 1. Induction of UPR and autophagy in MCF7 breast cancer cells. *A,* MCF7 cells were treated with 100 nmol/L, 1 μmol/L, and 5 μmol/L of Bortezomib and incubated at 37°C 5% CO_2 for 24 h. Levels of protein expression were measured by immunoblot analysis using antibodies against HIF1α, phospho-PERK(Thr980), phospho-eIF2α (Ser51), eIF2α ATF4, LC3B, and β-TUBULIN. *B,* MCF7 cells were treated with 100 nmol/L of Bortezomib for the indicated period of time. Levels of protein expression were measured by immunoblot analysis using antibodies against HIF1α, phospho-PERK(Thr980), phospho-eIF2α (Ser51), ATF4, LC3B, and β-TUBULIN. MDA-231 cells were treated with 100 nmol/L of Bortezomib for the indicated period of time. Levels of protein expression were measured by immunoblot analysis using antibodies against ATF4, LC3B, and β-tubulin. *C,* MCF7 cells were treated with 100 nmol/L, 1 μmol/L, and 5 μmol/L of Bortezomib and incubated for 24 h. Relative mRNA levels were measured by qPCR. $n = 3$; *, significance in two-tailed Student's *t* test; *, $P < 0.05$; **, $P < 0.005$; ***, $P < 0.0005$. *D,* MCF7 cells were treated with 100 nmol/L of Bortezomib for the indicated period of time. Relative mRNA levels were measured by qPCR. $n = 3$; *, significance in two-tailed Student's *t* test; *, $P < 0.05$; **, $P < 0.005$; ***, $P < 0.0005$. *Columns,* mean results representative of three similar experiments; *bars,* SE.

of HIF1α on the induction of ATF4 and LC3B, MCF7 cells transfected with RNAi against *HIF1α* were treated with 100 nmol/L of Bortezomib for 24 hours. There was no difference in induction of ATF4 and LC3B between HIF1α knockdown cells and SCR control (Fig. 2*A*).

Induction of ATF4 and LC3B by Bortezomib does not depend on activation of PERK. To directly determine the role of ATF4 in the cellular response to Bortezomib treatment, we compared gene expression in *ATF4* siRNA and control (SCR) siRNA–transfected cells treated with Bortezomib (100 nmol/L) for 24 hours. Transient transfection with siRNA duplexes specific to *ATF4* in Bortezomib-treated cells resulted in significantly reduced mRNA levels of *LC3B* (51% reduction; $P = 0.02$) and *ATF4* target gene *CHOP* (38% reduction) as measured by qPCR (Fig. 2*B*). Also, *ATF4* knockdown led to a significant reduction in ATF4 and LC3B protein levels compared with control siRNA (SCR)–transfected cells (Fig. 2*C*).

To determine a role of PERK activation versus ATF4 stabilization in Bortezomib-induced expression of LC3B, we transiently transfected cells with siRNA duplexes specific for PERK. No significant difference in *ATF4* and *LC3B* protein levels was observed between PERK siRNA and control (SCR) siRNA–transfected cells treated with Bortezomib (100 nmol/L) for 24 hours (Fig. 2*D*) and phosphorylation of eIF2α was maintained. mRNA levels of *CHOP* and *LC3B* were also not affected by PERK knockdown in Bortezomib-treated cells as measured by qPCR (Supplementary Fig. S1*A*). In contrast, Tunicamycin-treated PERK knockdown cells showed reduced phosphorylation of eIF2α and reduced protein levels of ATF4 compared with the control (SCR) Tunicamycin–treated cells (Fig. 2*D*).

Increased autophagy in Bortezomib-treated cells is dependent on up-regulation of LC3B by ATF4. We used synthetic siRNA duplexes to specifically inhibit LC3B expression in Bortezomib-treated cells and thus block the up-regulation of

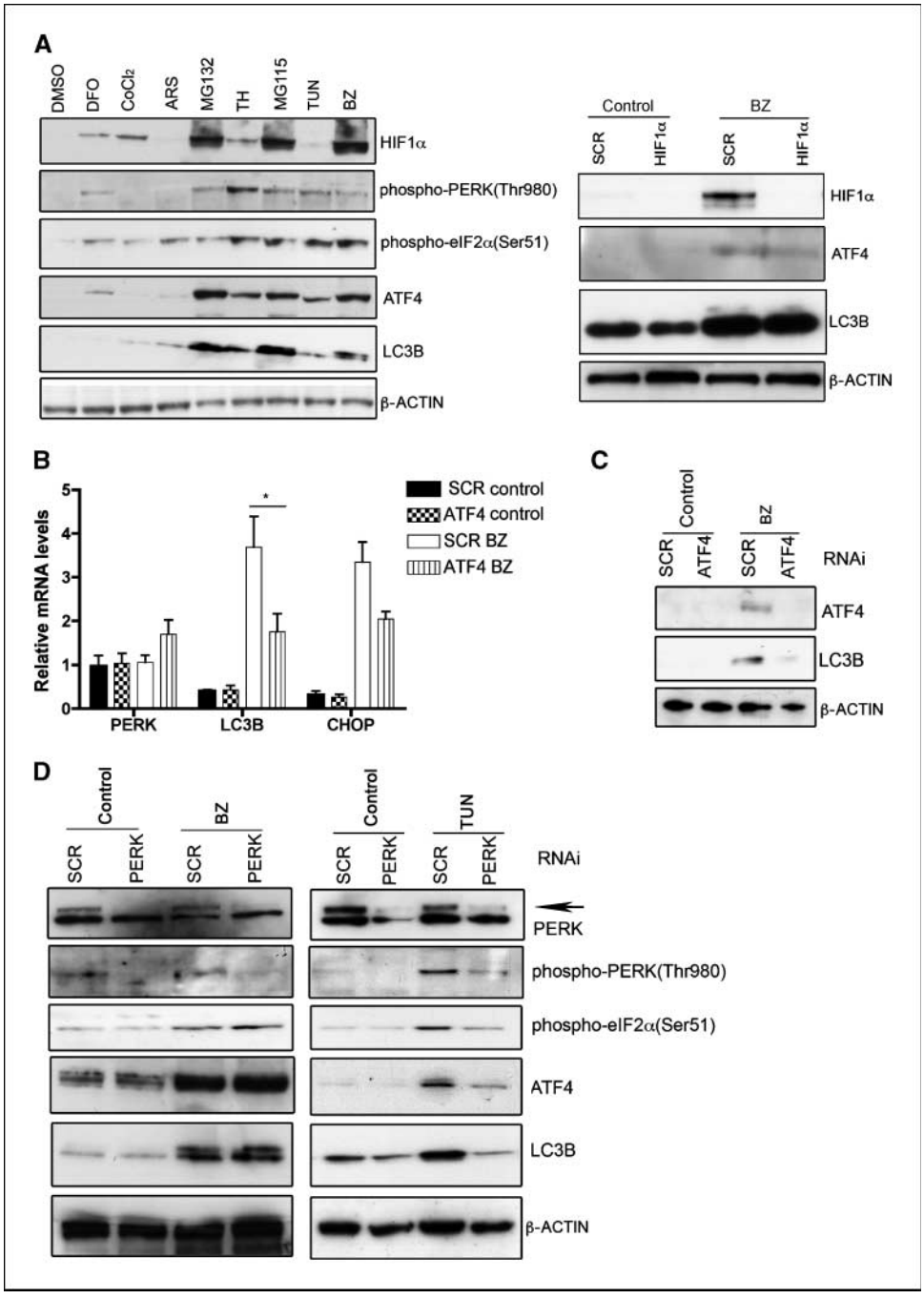

Figure 2. Induction of LC3B by Bortezomib (*BZ*) depends on proteolytic stabilization of ATF4. *A,* MCF7 cells were treated for 24 h with 40 μmol/L desferoxamine (*DFO*), 100 μmol/L $CoCl_2$, 5 μmol/L arsenite, 10 μmol/L MG132, 300 nmol/L Thapsigargin (*TH*), 5 μmol/L MG115, Tunicamycin (*TUN*) 5 μg/mL, and 100 nmol/L Bortezomib. Protein levels of HIF1α, phospho-PERK(Thr980), phospho-eIF2α (Ser51), ATF4, LC3B, and β-ACTIN were measured by immunoblot analysis. Levels of protein expression of HIF1α, ATF4, LC3B, and β-ACTIN are shown in cells transfected with RNAi against HIF1α and control (*SCR*). *B,* MCF7 cells transfected with RNAi against ATF4 and control (*SCR*) were treated with 100 nmol/L of Bortezomib for 24 h. Relative mRNA levels of PERK, LC3B, and CHOP were measured by qPCR. $n = 3$; *, significance in two-tailed Student's *t* test; *, $P < 0.05$; **, $P < 0.005$; ***, $P < 0.0005$. *Columns,* mean; *bars,* SE. *C,* MCF7 cells transfected with RNAi against ATF4 and control (*SCR*) were treated with 100 nmol/L of Bortezomib for 24 h. Protein levels were measured by immunoblot analysis. *D,* MCF7 cells transfected with RNAi specific to PERK and control (*SCR*) were treated with Bortezomib (100 nmol/L) and Tunicamycin (5μg/mL) for 24 h. Protein levels of ATF4, LC3B, and β-ACTIN were measured by immunoblot analysis. *Arrow,* specific band for PERK. Results here are representative of two similar experiments.

autophagy. MCF7 cells transiently transfected with siRNA duplexes, specific to LC3B, showed a significant reduction in LC3B protein levels, whereas induction of ATF4 and phosphorylation of eIF2α by Bortezomib were not affected (Fig. 3*A*).

To investigate if Bortezomib-induced protein levels of LC3B contribute to induction of autophagy, we performed immunostaining using an antibody against LC3B to visualize autophagosomes. MCF7 cells showed an increase in LC3B-positive foci after 24 hours of treatment with Bortezomib, the hallmark of autophagy, whereas ATF4 and LC3B knockdown cells failed to induce significant LC3B-positive foci (Fig. 3*B, C*, and *D*).

Cells treated with Bortezomib for 24 hours also showed a significant increase in lysosomal mass as determined by Lysotracker, a red fluorescent dye that stains acidic compartments in live cells (Fig. 3*B*). Moreover LC3B knockdown cells showed a decrease in the lysosomal compartment compared with SCR control cells when treated with Bortezomib (100 nmol/L), as detected by Lysotracker staining (Supplementary Fig. S1*B*).

HDAC6 is involved in Bortezomib-induced autophagy. As HDAC6 has emerged as an important factor required for autophagic degradation in cells with mutated UPS, we investigated whether HDAC6 was also important for the induction of autophagy in cells where the proteasome was inhibited by Bortezomib. HDAC6 knockdown in Bortezomib-treated cells resulted in reduced LC3B protein levels (Fig. 4*A*). There was no significant change in LC3B mRNA levels, and HDAC6 knockdown did not affect

induction of the UPR as measured by mRNA levels of *CHOP* (Fig. 4*B*). In MCF7 cells transiently transfected with siRNA duplexes specific for HDAC6 and treated with Bortezomib, autophagy levels were greatly reduced compared with control siRNA-transfected cells and visualized by LC3B immunostaining (Fig. 4*C*).

The role of UPR and autophagy in survival of MCF7 cells treated with Bortezomib. We analyzed the effects of Bortezomib on viability of MCF7 cells transfected with RNAi specific to *LC3B*, *ATF4*, *PERK*, or control SCR. The IC_{50} values for 72-hour treatment of Bortezomib, evaluated with a dose response assay (Fig. 5*A*), were as follows: SCR, 5.7 $\pm$ 0.1 nmol/L (n = 2); LC3B, 2.9 $\pm$ 0.1 nmol/L (n = 2); ATF4, 0.9 $\pm$ 0.1 nmol/L (n = 2); and siRNA PERK, 5.3 $\pm$ 0.1 nmol/L (n = 2), showing an increased sensitivity to Bortezomib in PERK, LC3B, and ATF4 siRNA–transfected cells (Fig. 5*A*). Next, we performed an MTS assay using the concentration of 100 nmol/L Bortezomib, previously used for the functional studies of ATF4 and other UPR markers. In this assay, we confirmed that ATF4 knockdown cells were more sensitive to Bortezomib treatment (45% $\pm$ 7.9%, P < 0.0001, at 48 hours and 26.8% $\pm$ 3.0%, P < 0.0001, at 72 hours; n = 6) compared with the viability of control siRNA SCR cells also treated with Bortezomib. They were also more sensitive to Bortezomib than LC3B (69.4% $\pm$ 8.7%, P < 0.0001, at 48 hours and 67.9% $\pm$ 10.2%, at 72-hour viability of siRNA SCR cells; n = 6) and PERK siRNA–transfected cells (74.9% $\pm$ 22.1%, P = 0.04, at 48 hours and 61.1% $\pm$ 20.1%, P < 0.0003, at 72-hour viability of siRNA SCR cells; n = 6; Fig. 5*B*).

The role of HDAC6 on proliferation in MCF7 cells treated with Bortezomib was assessed in a MTS assay. Cells lacking HDAC6 were significantly more sensitive at 24 hours (65% $\pm$ 16% viability of control siRNA SCR cells, P < 0.0001; n = 6) and at 48 hours (53% $\pm$ 16% viability of control siRNA SCR cells, P < 0.0001; n = 6) of Bortezomib treatment (Fig. 5*C*). MCF7 cells transfected with siRNA against *ATF4*, *LC3B*, and SCR control were counted after 24 hours, 48 hours without any treatment (Fig. 6*A*), or after exposure to Bortezomib (Fig. 6*B*). Cells lacking either LC3B or ATF4 were significantly more sensitive (79.5% $\pm$ 2.6%, P = 0.0006, and 50% $\pm$ 4%, P < 0.0001 viability of control siRNA SCR–transfected cells, respectively; n = 3) at 48 hours of Bortezomib treatment, with the loss of ATF4 resulting in the greatest sensitivity to Bortezomib (Fig. 6*B*). Thus, in all assays, ATF4 knockdown conferred the greatest sensitivity. We also investigated the effect on proliferation in MB MDA231 cells. The cells were counted after 24, 48, and 72 hours of treatment with Bortezomib (10 nmol/L). The loss of ATF4 or LC3B lead to a significant increase in sensitivity to Bortezomib compared with SCR control cells after 24 hours (65% $\pm$ 3%, P = 0.04, and 47.5% $\pm$ 2%, P = 0.0024, viability of control siRNA SCR–transfected cells, respectively; n = 3), 48 hours (34% $\pm$ 0.6%, P = 0.003, and 18.5% $\pm$ 1%, P = 0.0006, viability of control siRNA SCR–transfected cells, respectively; n = 3), and 72 hours (29.0% $\pm$ 4.0%, P = 0.02, and 13% $\pm$ 1%, P = 0.0006, viability of control siRNA SCR–transfected cells, respectively; n = 3; Fig. 6*C*), consistent with the MCF7 results.

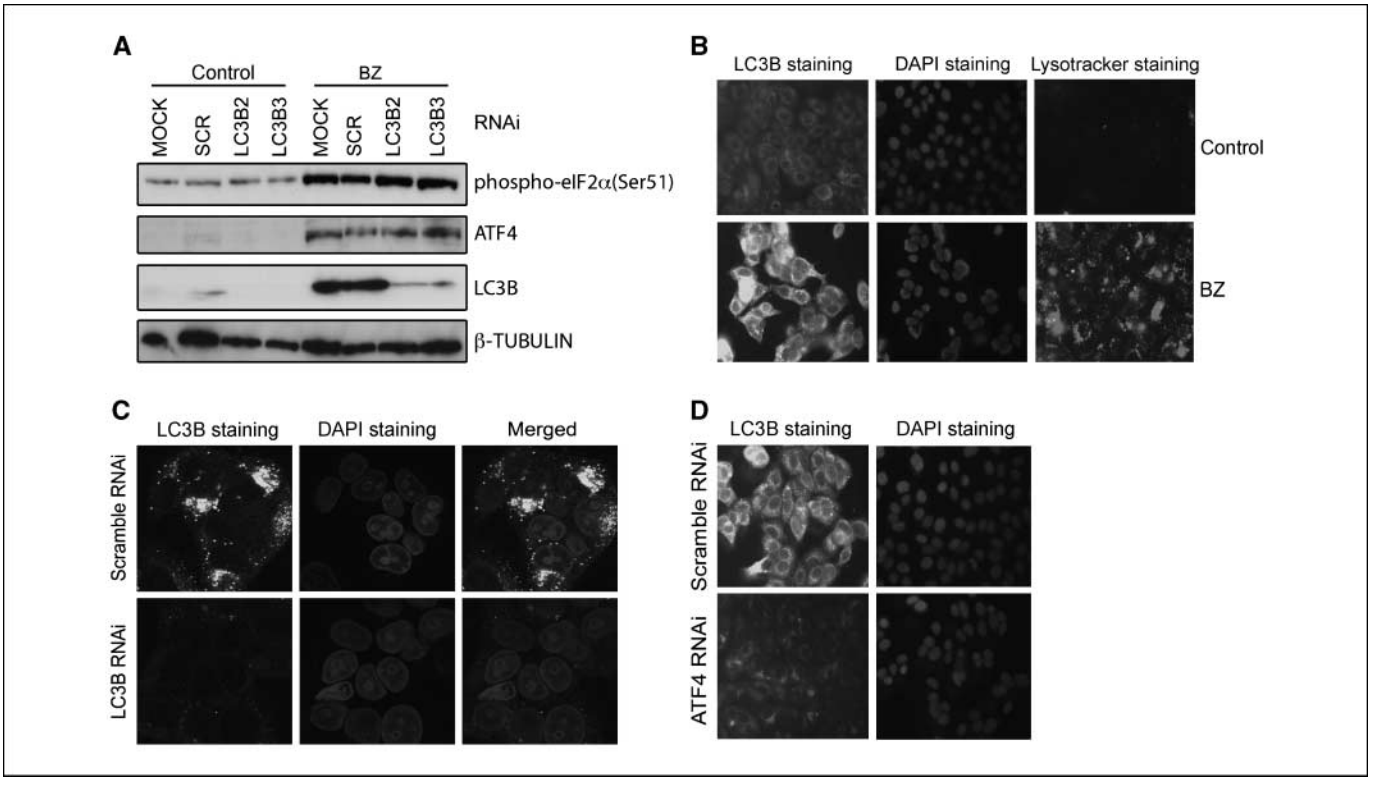

Figure 3. LC3B is a rate-limiting factor for the induction of autophagy in MCF7 cells treated with Bortezomib. *A,* MCF7 cells transfected with RNAi for LC3B and control (*SCR*) were treated with Bortezomib for 24 h. Two different siRNA duplexes against LC3B were used, 2 and 3. Protein levels were measured by immunoblot analysis using antibodies against phospho-eIF2α (Ser51), ATF4, LC3B, and β-TUBULIN. *B,* MCF7 cells were treated with 100 nmol/L of Bortezomib for 24 h and stained with antibody against LC3B. 4′,6-Diamidino-2-phenylindole (DAPI) nuclear counterstaining and Lysotracker staining are shown. *C,* MCF7 cells transfected with RNAi against LC3B and control (SCR) were treated with 100 nmol/L of Bortezomib for 24 h and stained with antibody against LC3B. DAPI nuclear counterstaining is shown. *D,* MCF7 cells transfected with RNAi against ATF4 and control (SCR) were treated with 100 nmol/L of Bortezomib for 24 h and stained with antibody against LC3B. DAPI nuclear counterstaining is shown.

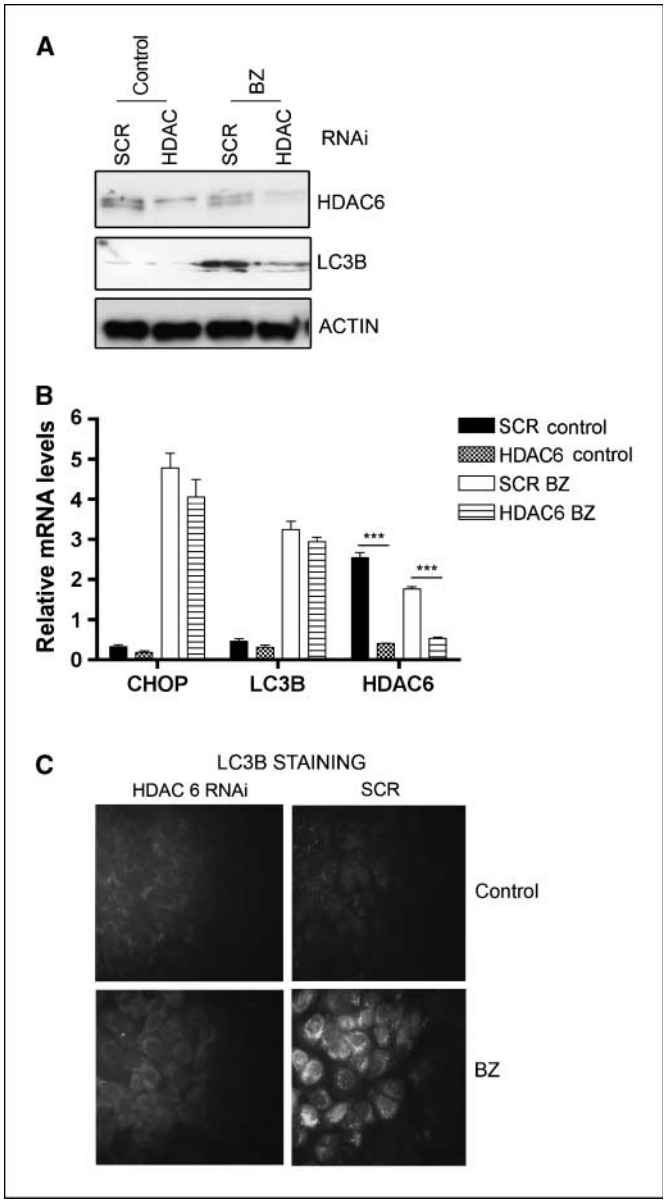

Figure 4. Induction of autophagy in MCF7 cells treated with Bortezomib depends on HDAC6. *A,* MCF7 cells transfected with RNAi against HDAC and control (*SCR*) were treated with 100 nmol/L of Bortezomib for 24 h. Protein levels were measured by immunoblotting using antibodies against HDAC6, LC3B, and β-ACTIN. *B,* MCF7 cells transfected with RNAi against HDAC and SCR were treated with 100 nmol/L of Bortezomib for 24 h. Relative mRNA levels of CHOP and LC3B were measured by quantitative PCR. $n = 3$; *, significance in two-tailed Student's t test; *, $P < 0.05$; **, $P < 0.005$; ***, $P < 0.0005$; *columns,* mean of three similar experiments; *bars,* SE. *C,* MCF7 cells transfected with RNAi against HDAC6 and SCR were treated with 100 nmol/L of Bortezomib for 24 h and stained with antibody against HDAC6. Results here represent three similar experiments.

We performed FACS analysis to investigate cell death after 24, 48, and 72 hours of treatment with Bortezomib (100 nmol/L) in MCF7 cells transfected withRNAi specific to ATF4, LC3B, and SCR control. The loss of LC3B or ATF4 was associated with a significant increase in dead cells staining for both Annexin V and propidium iodide with respect to SCR control cells after 48 and 72 hours of treatment (Fig. 6*D*).

Discussion

Bortezomib is a selective and potent proteasome inhibitor currently available for treatment of multiple myeloma and several solid tumors but did not show activity in breast cancer (1, 2). Clinical trials showed no objective response in heavily treated

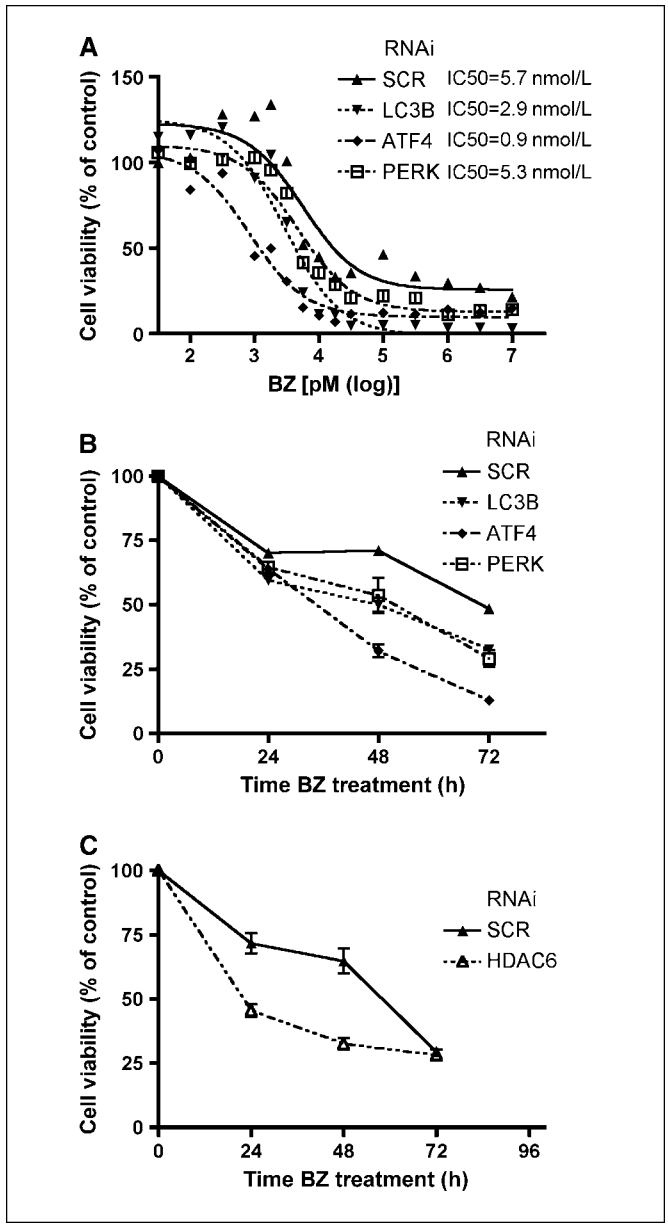

Figure 5. The role of UPR and autophagy in survival of MCF7 cells treated with Bortezomib. *A,* dose response assay. MCF7 cells were transfected with RNAi against SCR, LC3B, ATF4, and PERK. Sixteen hours later, cells were seeded, allowed to recover for 8 h, and treated with a range of Bortezomib concentration (1 nmol/L to 10 μmol/L) for 72 h. Results here represent two similar experiments. *B,* proliferation assay. MCF7 cells were seeded and transfected with RNAi against SCR, LC3B, ATF4, and PERK. Sixteen hours later, cells were seeded, allowed to recover for 8 h, and treated with Bortezomib (100 nmol/L). Proliferation was measured with MTS reagent after the indicated period of time. Results here represent three similar experiments. For each time point: $n = 3$; *points,* mean; *bars,* SE. *C,* proliferation assay. MCF7 cells were transfected with RNAi against HDAC6. Sixteen hours later, cells were seeded, allowed to recover for 8 h, and treated with Bortezomib (100 nmol/L). Proliferation was measured with MTS reagent after the indicated period of time. *Points,* mean of three similar experiments ($n = 3$); *bars,* SE.

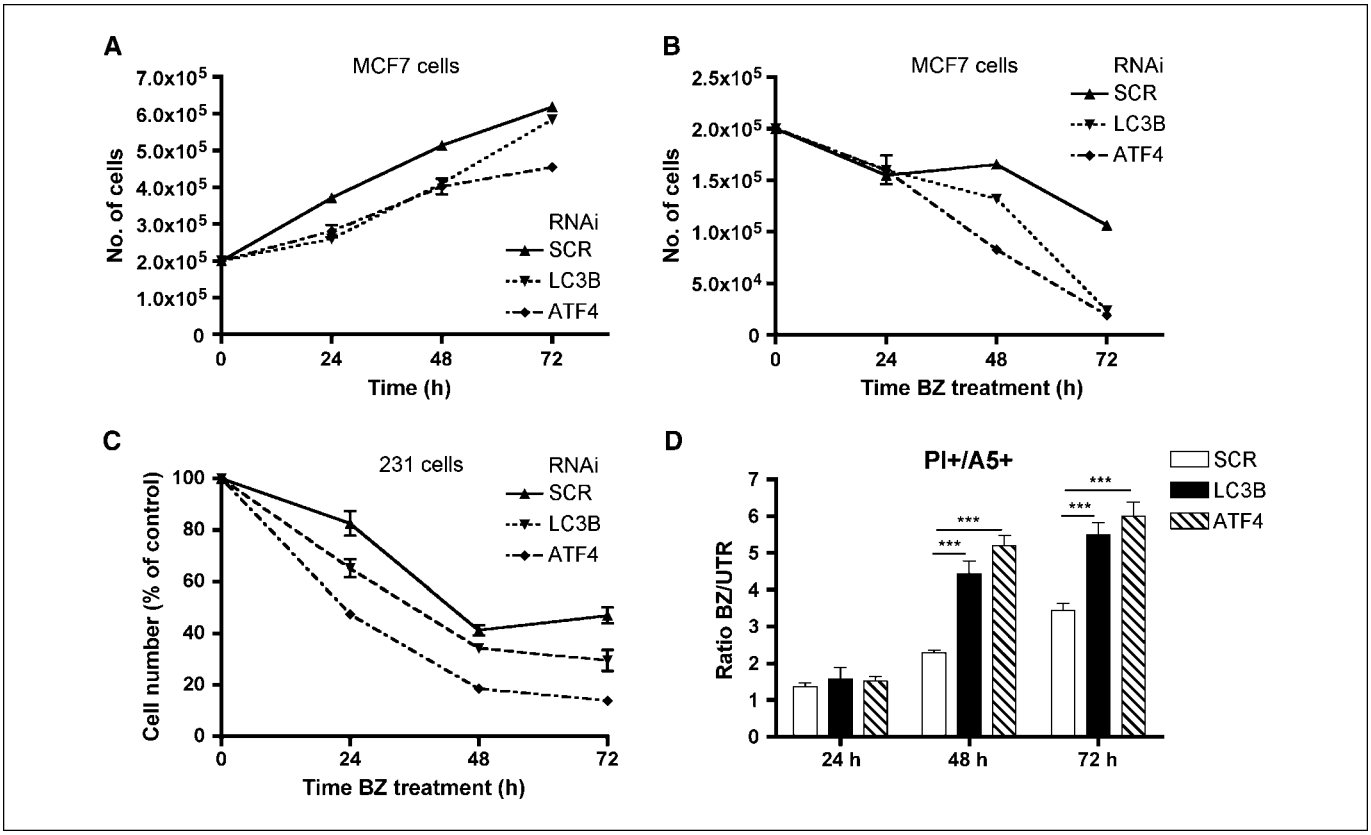

Figure 6. Cell growth of MCF7 cells treated with Bortezomib. *A,* MCF7 cells were transfected with RNAi against SCR, LC3B, ATF4. Sixteen hours later, cells were seeded in 10-cm Petri dishes (200.000 cells per dish), allowed to recover for 8 h, and counted after indicated period of time. *B,* MCF7 cells were transfected with RNAi against SCR, LC3B, ATF4. Sixteen hours later, cells were seeded in 10-cm Petri dishes (200.000 cells per dish), allowed to recover for 8 h, and treated with 100 nmol/L of Bortezomib. The number of viable cells was counted after indicated period of time. *Points,* mean of three similar experiments ($n = 3$); *bars,* SE. *C,* MB MDA 231 cells were transfected with RNAi against SCR, LC3B, and ATF4. Sixteen hours later, cells were seeded in 10-cm Petri dishes (200.000 cells per dish), allowed to recover for 8 h, and treated with 100 nmol/L of Bortezomib. The number of viable cells was counted after indicated period of time. *Points,* mean of three similar experiments ($n = 3$); *bars,* SE. *D,* FACS analysis was performed. MCF7 cells were stained with propidium iodide (*PI*) and Annexin 5 (*A5*). $n = 3$; *, significance in Anova test; *, $P < 0.05$; **, $P < 0.005$; ***, $P < 0.0005$.

patients with metastatic breast cancer using Bortezomib as single agent (20, 21).

Here, we investigated mechanisms of resistance to Bortezomib in MCF7 breast cancer cells, which have been previously described as cells relatively resistant to Bortezomib, and with high proteasome activity (22). Proteasome inhibition leads to the accumulation of misfolded proteins in cells resulting in endoplasmic reticulum stress (23). Endoplasmic reticulum stress activates the UPR, a cellular adaptive response that leads to an inhibition of protein translation through the phosphorylation of eIF2α. *In vivo* studies have shown that PERK-eIF2α-ATF4 pathway plays an important role in tumor development as xenograft tumors derived from cells with an inactivated PERK-eIF2α-ATF4 are smaller and grow more slowly than wild-type cells (24). It has been shown that Bortezomib treatment induces the UPR in myeloma (25) and pancreatic cells (4, 26), and here, we show that this pathway was also activated in MCF7 breast cancer cells with induction of ATF4 and ATF4-related genes. ATF4 is a mediator of the integrated stress response and it plays a key role in regulating the expression of many genes encoding chaperones, factors involved in amino acid metabolism and transport and redox homeostasis (6, 27, 28). Consequently, cells lacking ATF4 showed increased susceptibility to endoplasmic reticulum and other stressors, including amino acid deprivation and oxidative stress (27), so there are several possible mechanisms involved in survival. Although we could detect phosphorylation of eIF2α and PERK in Bortezomib-treated cells, and with different endoplasmic reticulum stressors, there was a much stronger induction of ATF4 in cells treated with proteasomal inhibitors. Furthermore, knockdown of PERK inhibited induction of ATF4 by other stimuli but not Bortezomib. Cumulatively, this novel observation indicates that the main mechanism through which Bortezomib induces ATF4 is protein stabilization due to the proteasome inhibition, rather than the activation of PERK.

It has been reported that in pancreatic cells Bortezomib treatment did not induce phosphorylation of eIF2α, but two other studies showed that proteasomal inhibitors treatment lead to autophosphorylation of PERK in a head and neck squamous cell carcinoma model and eIF2α phosphorylation in mouse embryonic fibroblasts (29, 30), which shows the heterogeneity and complexity of the UPR in Bortezomib-treated cells. In our study, eIF2α phosphorylation was induced by Bortezomib in the PERK siRNA–treated cells, implying another kinase is activated.

Recent findings now suggest that the endoplasmic reticulum stress is a potent inducer of autophagy, although the mechanism is not clear (7, 8). Here, we show that Bortezomib induces LC3B, at both the protein and mRNA level by a mechanism involving ATF4. Induction of LC3B by ATF4 in Bortezomib-treated cells was

independent of PERK. We also show a novel role for ATF4 in regulating protein levels of LC3B, which were rate limiting for the induction of autophagy in Bortezomib-treated cells, and that autophagy was impaired in cells lacking ATF4.

The UPR is implicated in both a prosurvival response, to maintain cellular homeostasis, and in apoptotic cell death when responses are not sufficient to relieve endoplasmic reticulum stress (31). The loss of ATF4 and LC3B was associated with an increase in cell death, suggesting that ATF4 and autophagy play a prosurvival role under Bortezomib treatment. However, the precise mechanism of Bortezomib-induced endoplasmic reticulum–dependent cell death is still unclear and likely to be cell type specific (32). Several studies support the hypothesis that Bortezomib sensitizes cancer cells to endoplasmic reticulum stress–mediated apoptosis (4, 29). However, recent findings suggest that massive induction of endoplasmic reticulum stress response and autophagy, by the combination of Bortezomib with other stresses, such as hypoxia, may drive tumor cells into necrosis (32, 33). Interestingly, it was previously shown that the UPR is also involved in resistance mechanisms to a variety of agents, including the topoisomerase inhibitor etoposide (34). Other evidence showed that ATF4 could be induced by cisplatin and overexpression of ATF4 conferred cisplatin resistance in cells (35). Furthermore, the UPR has been shown to induce the multidrug resistance gene 1 in human cancer cell lines (36).

In our work, we investigated the role of UPR in resistance of MCF7 cells to Bortezomib, by the induction of prosurvival pathways that could help to relieve the protein overload. Stabilization of the ATF4 protein lead to the induction of LC3B; therefore, we also investigated a role of autophagy in Bortezomib resistance. LC3B knockdown cells showed impaired autophagy and were more sensitive to Bortezomib, suggesting that the induction of LC3B through ATF4 is an important mechanism of Bortezomib resistance. Cells lacking ATF4 were more sensitive to Bortezomib than those lacking PERK or LC3B, suggesting that ATF4 plays a key role in protecting cells from death under Bortezomib treatment, through additional autophagy-independent mechanisms.

Recent evidence has shown that a proteasome-independent pathway eliminates unfolded polyubiquitinated proteins, known as the aggresome pathway, is linked to autophagy. HDAC6, a microtubule-associated deacetylase, couples misfolded polyubiquitinated proteins to the dynein motor complex, resulting in the formation of aggresomes and clearance by autophagy (15). It has been shown that autophagy can act as a compensatory degradation system when the UPS is impaired by genetic mutations in *Drosophila*, and that HDAC6 is an essential mechanistic link in this compensatory interaction (37). Inhibition of both the proteasome and HDAC6 by tubacin induced accumulation of ubiquitinated proteins and enhanced toxicity in multiple myeloma and ovarian cancer cells, although the mechanism linking the two was not known (38). We have shown that the loss of HDAC6 is associated with strong reduction of the LC3B protein but did not have any effect on mRNA levels of *LC3B* in Bortezomib-treated cells. Moreover, we observed that HDAC6 knockdown cells were more sensitive to Bortezomib treatment. This may be directly linked with the down-regulation of LC3B in cells lacking HDAC6 but requires further study. From a clinical point of view, it would be an attractive possibility to target UPR in combination with Bortezomib to enhance the response of breast cancer to Bortezomib, and sensitize to environmental stress that normally occurs in solid tumors. Although currently no specific inhibitors of UPR are clinically available, we are screening for such compounds. Thus, autophagy and the HDAC6 pathway are important targets for synergistic therapy and combinations of drugs blocking these pathways represents a testable approach to sensitize cancer cells to Bortezomib.

Disclosure of Potential Conflicts of Interest

No potential conflicts of interest were disclosed.

Acknowledgments

Received 7/24/08; revised 2/10/09; accepted 3/9/09; published OnlineFirst 5/5/09.

The costs of publication of this article were defrayed in part by the payment of page charges. This article must therefore be hereby marked *advertisement* in accordance with 18 U.S.C. Section 1734 solely to indicate this fact.

Cancer Research UK, Cremona Breast Unit, Millennium Pharmaceuticals, Inc. (Cambridge, MA).

References

1. Adams J, Palombella VJ, Sausville EA, et al. Proteasome inhibitors: a novel class of potent and effective antitumor agents. Cancer Res 1999;59:2615–22.
2. Adams J. The development of proteasome inhibitors as anticancer drugs. Cancer Cell 2004;5:417–21.
3. Caravita T, de Fabritiis P, Palumbo A, Amadori S, Boccadoro M. Bortezomib: efficacy comparisons in solid tumors and hematologic malignancies. Nat Clin Pract Oncol 2006;3:374–87.
4. Nawrocki ST, Carew JS, Pino MS, et al. Bortezomib sensitizes pancreatic cancer cells to endoplasmic reticulum stress-mediated apoptosis. Cancer Res 2005; 65:11658–66.
5. Rzymski T, Harris AL. The unfolded protein response and integrated stress response to anoxia. Clin Cancer Res 2007;13:2537–40.
6. Harding HP, Zhang Y, Ron D. Protein translation and folding are coupled by an endoplasmic-reticulum-resident kinase. Nature 1999;397:271–4.
7. Yorimitsu T, Klionsky DJ. Endoplasmic reticulum stress: a new pathway to induce autophagy. Autophagy 2007;3:160–2.
8. Yorimitsu T, Nair U, Yang Z, Klionsky DJ. Endoplasmic reticulum stress triggers autophagy. J Biol Chem 2006; 281:30299–304.
9. Talloczy Z, Jiang W, Virgin HWt, et al. Regulation of starvation- and virus-induced autophagy by the eIF2α kinase signaling pathway. Proc Natl Acad Sci U S A 2002; 99:190–5.
10. Kouroku Y, Fujita E, Tanida I, et al. ER stress (PERK/eIF2α phosphorylation) mediates the polyglutamine-induced LC3 conversion, an essential step for autophagy formation. Cell Death Differ 2007;14:230–9.
11. Shimizu S, Kanaseki T, Mizushima N, et al. Role of Bcl-2 family proteins in a non-apoptotic programmed cell death dependent on autophagy genes. Nat Cell Biol 2004;6:1221–8.
12. Shintani T, Klionsky DJ. Autophagy in health and disease: a double-edged sword. Science 2004;306:990–5.
13. Shao Y, Gao Z, Marks PA, Jiang X. Apoptotic and autophagic cell death induced by histone deacetylase inhibitors. Proc Natl Acad Sci U S A 2004;101:18030–5.
14. Haggarty SJ, Koeller KM, Wong JC, Grozinger CM, Schreiber SL. Domain-selective small-molecule inhibitor of histone deacetylase 6 (HDAC6)-mediated tubulin deacetylation. Proc Natl Acad Sci U S A 2003;100:4389–94.
15. Rodriguez-Gonzalez A, Lin T, Ikeda AK, Simms-Waldrip T, Fu C, Sakamoto KM. Role of the aggresome pathway in cancer: targeting histone deacetylase 6-dependent protein degradation. Cancer Res 2008;68: 2557–60.
16. Rzymski T, Paantjens A, Bod J, Harris AL. Multiple pathways are involved in the anoxia response of SKIP3 including HuR-regulated RNA stability, NF-κB and ATF4. Oncogene 2008;27:4532–43.
17. Birle DC, Hedley DW. Suppression of the hypoxia-inducible factor-1 response in cervical carcinoma xenografts by proteasome inhibitors. Cancer Res 2007; 67:1735–43.
18. Shin DH, Chun YS, Lee DS, Huang LE, Park JW. Bortezomib inhibits tumor adaptation to hypoxia by stimulating the FIH-mediated repression of hypoxia-inducible factor-1. Blood 2008;111:3131–6.
19. Giatromanolaki A, Koukourakis MI, Pezzella F, et al. Expression of prolyl-hydroxylases PHD-1, 2 and 3 and of the asparagine hydroxylase FIH in non-small cell lung cancer relates to an activated HIF pathway. Cancer Lett 2008;262:87–93.
20. Engel RH, Brown JA, Von Roenn JH, et al. A phase II study of single agent bortezomib in patients with

metastatic breast cancer: a single institution experience. Cancer Invest 2007;25:733–7.
21. Yang CH, Gonzalez-Angulo AM, Reuben JM, et al. Bortezomib (VELCADE) in metastatic breast cancer: pharmacodynamics, biological effects, and prediction of clinical benefits. Ann Oncol 2006;17:813–7.
22. Codony-Servat J, Tapia MA, Bosch M, et al. Differential cellular and molecular effects of bortezomib, a proteasome inhibitor, in human breast cancer cells. Mol Cancer Ther 2006;5:665–75.
23. Lee AH, Iwakoshi NN, Anderson KC, Glimcher LH. Proteasome inhibitors disrupt the unfolded protein response in myeloma cells. Proc Natl Acad Sci U S A 2003;100:9946–51.
24. Bi M, Naczki C, Koritzinsky M, et al. ER stress-regulated translation increases tolerance to extreme hypoxia and promotes tumor growth. EMBO J 2005;24:3470–81.
25. Obeng EA, Carlson LM, Gutman DM, Harrington WJ, Jr., Lee KP, Boise LH. Proteasome inhibitors induce a terminal unfolded protein response in multiple myeloma cells. Blood 2006;107:4907–16.
26. Nawrocki ST, Carew JS, Dunner K, Jr., et al. Bortezomib inhibits PKR-like endoplasmic reticulum (ER) kinase and induces apoptosis via ER stress in human pancreatic cancer cells. Cancer Res 2005;65:11510–9.
27. Harding HP, Zhang Y, Zeng H, et al. An integrated stress response regulates amino acid metabolism and resistance to oxidative stress. Mol Cell 2003;11:619–33.
28. Blais JD, Filipenko V, Bi M, et al. Activating transcription factor 4 is translationally regulated by hypoxic stress. Mol Cell Biol 2004;24:7469–82.
29. Fribley A, Zeng Q, Wang CY. Proteasome inhibitor PS-341 induces apoptosis through induction of endoplasmic reticulum stress-reactive oxygen species in head and neck squamous cell carcinoma cells. Mol Cell Biol 2004;24:9695–704.
30. Jiang HY, Wek RC. Phosphorylation of the α-subunit of the eukaryotic initiation factor-2 (eIF2α) reduces protein synthesis and enhances apoptosis in response to proteasome inhibition. J Biol Chem 2005;280:14189–202.
31. Kim R, Emi M, Tanabe K, Murakami S. Role of the unfolded protein response in cell death. Apoptosis 2006;11:5–13.
32. Fels DR, Ye J, Segan AT, et al. Preferential cytotoxicity of bortezomib toward hypoxic tumor cells via overactivation of endoplasmic reticulum stress pathways. Cancer Res 2008;68:9323–30.
33. Amaravadi RK, Thompson CB. The roles of therapy-induced autophagy and necrosis in cancer treatment. Clin Cancer Res 2007;13:7271–9.
34. Reddy RK, Mao C, Baumeister P, Austin RC, Kaufman RJ, Lee AS. Endoplasmic reticulum chaperone protein GRP78 protects cells from apoptosis induced by topoisomerase inhibitors: role of ATP binding site in suppression of caspase-7 activation. J Biol Chem 2003;278:20915–24.
35. Tanabe M, Izumi H, Ise T, et al. Activating transcription factor 4 increases the cisplatin resistance of human cancer cell lines. Cancer Res 2003;63:8592–5.
36. Comerford KM, Wallace TJ, Karhausen J, Louis NA, Montalto MC, Colgan SP. Hypoxia-inducible factor-1-dependent regulation of the multidrug resistance (MDR1) gene. Cancer Res 2002;62:3387–94.
37. Boyault C, Sadoul K, Pabion M, Khochbin S. HDAC6, at the crossroads between cytoskeleton and cell signaling by acetylation and ubiquitination. Oncogene 2007;26:5468–76.
38. Bazzaro M, Lin Z, Santillan A, et al. Ubiquitin proteasome system stress underlies synergistic killing of ovarian cancer cells by bortezomib and a novel HDAC6 inhibitor. Clin Cancer Res 2008;14:7340–7.